Matter rogue waves

Yu. V. Bludov,[1] V. V. Konotop,[2,3] and N. Akhmediev[4]
[1]*Centro de Física, Universidade do Minho, Campus de Gualtar, Braga 4710–057, Portugal*
[2]*Centro de Física Teórica e Computacional, Universidade de Lisboa, Complexo Interdisciplinar, Avenida Professor Gama Pinto 2, Lisboa 1649-003, Portugal*
[3]*Departamento de Física, Universidade de Lisboa, Campo Grande, Edifício C8, Piso 6, Lisboa 1749-016, Portugal*
[4]*Optical Sciences Group, Research School of Physics and Engineering, The Australian National University, Canberra, ACT 0200, Australia*
(Received 30 June 2009; published 15 September 2009)

We predict the existence of rogue waves in Bose-Einstein condensates either loaded into a parabolic trap or embedded in an optical lattice. In the latter case, rogue waves can be observed in condensates with positive scattering length. They are immensely enhanced by the lattice. Local atomic density may increase up to tens times. We provide the initial conditions necessary for the experimental observation of the phenomenon. Numerical simulations illustrate the process of creation of rogue waves.

DOI: 10.1103/PhysRevA.80.033610 PACS number(s): 03.75.Kk, 03.75.Lm, 67.85.Hj

I. INTRODUCTION

Rogue waves are strong wavelets that may appear in the ocean when appropriate conditions are met [1]. These waves can be two, three, or even more times higher than the average wave crests [2]. The resulting peak may reach the height of 20–30 m and by some estimates even 60 m. Clearly, these giants would be very dangerous if it appeared on the path of an ocean liner (and that is why they are also called "killer" waves). Many cases of such encounters are described and even photos are presented [3]. The first measurement of the rogue wave in the open ocean is taken on the oil platform in Norway in 1995 [3], thus confirming that the rogue waves are indeed a reality rather than myths spread by sailors. Detailed studies in the frame of the program "MAXWAVE" that include satellite data showed that waves with the height of 25 m are not unusual [4].

There is a variety of mathematical descriptions of waves in the ocean [5]. One of them, related to deep ocean waves, is based on the nonlinear Schrödinger (NLS) equation [6]. Particular explanations also vary [7]. The basic phenomenon related to this description is Benjamin-Fair (or Bespalov-Talanov) [8] instability or more generally speaking modulation instability (MI). Peregrine first noticed that such instability can be responsible for a quick increase in the wave amplitude in the ocean [9]. There is wide range of initial frequencies that are amplified due to MI, and the resulting waves can reach amplitudes substantially higher than those in the initial conditions. In particular, zero-frequency perturbation leads to the wavelet with highest amplitude that is known as Peregrine soliton [9]. The latter is the solution localized in two directions and described analytically by the rational expression [see Eq. (2) below]. Recent studies showed that even higher amplitudes can be reached due to the interaction of several MI components [10] or due to the wavelets that are described by the higher-order rational solution [11].

Recently, the notion of the rogue wave has been transferred into the realm of nonlinear optics [12]. Experimental studies have shown that continuous-wave laser radiation in optical fibers splits into separate pulses and those pulses can reach very high amplitudes [12]. Indeed, the wave propagation in optical fibers at certain frequencies is described by the NLS equation or its modification, and the nature of appearance of high peaks could be very similar to the peaks in the open ocean. Moreover, due to random modulations of the initial carrier wave in a fiber, the high peaks at the output also arrive randomly just like in the ocean.

There are at least two fundamental reasons for great interest in generating rogue waves in laboratory conditions. First, this opens possibilities for detailed studies of their properties as well as testing applicability of the mathematical models developed for their descriptions (something unthinkable in the natural conditions). Second, being an essentially nonlinear phenomenon, rogue waves allow us to understand deeply the nature and the dynamics of instabilities in nonlinear systems. Thus, the natural question that appears is whether the rogue waves can be observed in other (than ocean or optical fibers) physical media.

The goal of this work is to give the positive answer to this question by showing that rogue waves are also rather natural in the microworld. Namely, they can be observed in Bose-Einstein condensates (BECs). The physical reasons for this are twofold. First, BEC represents a fluid, which in the mean-field approximation is accurately described by the Gross-Pitaevskii (GP), i.e., by the NLS equation [13]. Second, due to the two-body interactions, BEC is intrinsically a nonlinear system. Moreover, a BEC has great advantages compared to other nonlinear systems. Indeed, the nonlinear interactions can be experimentally managed by means of the Feshbach resonance [14], while the effective atomic mass and the stability properties can be varied with help of the optical lattice (OL) [15]. The suitable initial conditions can be created using phase and density engineering. In other words, rogue waves in BECs appear to be well controllable objects.

II. MODEL

To begin with, we start with the one-dimensional (1D) GP equation,

$$i\psi_t = -\psi_{xx} + \sigma|\psi|^2\psi - ig|\psi|^4\psi, \qquad (1)$$

where $\sigma=\text{sgn}(a_s)$ and a_s is the scattering length. In Eq. (1) we have explicitly included the dissipative term due to inelastic three-body interaction whose strength is characterized by $g>0$ [16]. This last point is of special relevance as the rogue waves correspond to a giant increase in the local density when the impact of the three-body collisions can become dominant.

Besides the inelastic three-body interactions in a real experimental situation relevant for the BEC applications, one has to also take into account a trap potential [see, e.g., the models (4) and (6) below]. This makes the problem very different from the analytically solvable NLS equation. Nevertheless, it is natural to expect that using the exact solution for the NLS rogue wave, one can guess the proper initial conditions, giving rise for the giant density enhancement in a realistic mean-field model of a BEC.

Therefore, we start by recalling that when $\sigma=-1$ and $g=0$, Eq. (1) possesses an exact analytic solution [9],

$$\psi_0(x,t) = \rho(x,t)e^{i\theta(x,t)} = \left(1 - 4\frac{1+2it}{1+2x^2+4t^2}\right)e^{it}, \qquad (2)$$

with the density ρ^2 and the phase distribution θ at each instant of time determined directly from this formula. Let us outline the physical properties of the field distribution (2), distinguishing it out of the large class of initial conditions leading to modulational instability. First, we observe that this is a solution with the mean density $n_0=1$, in which the domains of the high density $n(x,t)\equiv|\psi_0|^2>1$ and of the low density $n(x,t)<1$ are spatially separated at any time, being respectively $|x|<\sqrt{(1+4t^2)/2}$ and $|x|>\sqrt{(1+4t^2)/2}$. Second, the initial amplitude and phase modulation provide that the (superfluid) current density $j(x,t)\equiv i(\psi\bar{\psi}_x-\bar{\psi}\psi_x)=64xt/(1+2x^2+4t^2)^2$ is positive (negative) for all $x<0$ ($x>0$), i.e., the density excitations move toward (outward) the center $x=0$ at any instant of time $t<0$ ($t>0$). The amplitude of the solution (2) has its maximum at $t=0$ (see Fig. 1(a)), where the current density is zero $j(0,t)=0$ at any time.

Thus, turning to discussion of possible implementation of the matter rogue waves, we have to look for the initial conditions leading to dynamics which would closely resemble the physical behavior described above. While in any experiment the time is considered positive, to avoid introducing a time shift in Eq. (2), which would be less convenient for the analytical arguments, we assume that the experiment starts at initial time $t_i<0$. Moreover, we assume that $|t_i|\gg 1$, i.e., the initial homogeneous density distribution is only weakly modulated. Then the initial condition can be approximated by

$$\rho_i^2 = 1 + \frac{4(2t_i^2 - x^2)}{(2t_i^2 + x^2)^2} \quad \text{and} \quad \theta_i = t_i - \frac{4t_i}{x^2 + 2t_i^2}. \qquad (3)$$

More generally, this is the case where initially the following properties are satisfied: $\theta_{xx}(x,t_i)\ll\theta_x(x,t_i)\ll\theta_t(x,t_i)$ and, thus, one can neglect the kinetic energy. This readily gives the useful link $\theta_t(x,t_i)\approx\rho^2(x,t_i)$.

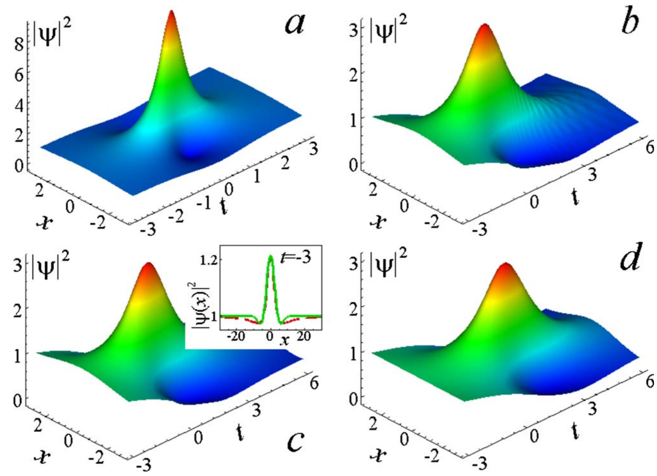

FIG. 1. (Color online) Evolution of the atomic density according to (a) the exact solution (2), (b) TF approximation with $\nu_i=0.02$, (c) "Mexican hat," and (d) uniform $\rho_i^2=1$ initial conditions. In (b), (c), and (d), the initial phase distribution θ_i is taken from Eq. (3). The initial time is $t_i=-3$. The inset in (c) shows the initial densities obtained from Eq. (2) (dashed line) and from the "Mexican hat" approximation ψ_{MH} (solid line). In (b), (c), and (d), we used $g=0.05$.

Now, let us consider preparation of the optimal initial conditions for observing rogue waves. We concentrate on the atomic density, assuming that the initial phase distribution θ_i is obtained using the phase imprinting technique [17]. The main difficulty in preparation of the respective initial state arises from the attractive interactions. The latter requires loading the condensate into a modulationally unstable state. Therefore, we take advantage of the Feshbach management [14], allowing one to change abruptly the sign of the scattering length at $t=t_i$. More specifically, at $t<t_i$ we consider the condensate having a positive scattering length, whose absolute value could be different from the one exploited in the attractive regime. Thus, we assume that at $t<t_i$ a condensate with $\sigma=\sigma_i>0$ (generally speaking $\sigma_i\neq 1$) is loaded into a parabolic trap ν^2x^2, where the dimensionless linear oscillator frequency ν is assumed to be small enough, or more specifically $t_i\nu\ll 1$. In order to create the distribution ρ_i given by Eq. (3), one also has to impose a potential $V_0(x)$ that provides necessary modulations specified below. Then the stationary state of such BEC is determined from the stationary GP equation

$$\mu\psi_i = -\psi_{i,xx} + V_0(x)\psi_i + \nu^2x^2\psi_i + \sigma_i|\psi_i|^2\psi_i, \qquad (4)$$

where μ is the chemical potential.

Let us now choose $V_0(x)=\mu-\sigma_i\rho_i^2(x)$. Then $V_0(x)$ is localized on the scale $|x|\lesssim t_i$ as it follows from Eq. (4). Recalling that the initial condition we are interested in corresponds to the negligible kinetic energy, we can find ψ_i in the Thomas-Fermi (TF) approximation: $|\psi_{TF}|^2=\rho_i^2-\nu_i^2x^2$. This is valid for $|x|<\tilde{x}$, where $\tilde{x}$ is the positive zero of $|\psi_{TF}|^2$, and $\nu_i=\nu/\sqrt{\sigma_i}$. Taking into account that at $|t_i|\gg 1$ the distribution $\rho_i\sim 1$, we make the standard estimate $\tilde{x}\approx\nu_i^{-1}$. Then the number of atoms loaded into the trap is $\mathcal{N}\approx\int_{-\tilde{x}}^{\tilde{x}}|\psi_{TF}|^2dx\sim\frac{4}{3}\tilde{x}$.

Generally speaking experimental creation of the trap potential $V_0(x)$ with $\rho_i^2(x)$ given by Eq. (3) can be not easy. It turns out however that excitation of a rogue wave can be implemented using initial distributions, which on the one hand are experimentally feasible and on the other hand closely mimic the "ideal" exact density (3). These cases require numerical study, which is performed in the next section.

III. ROGUES WAVES IN HOMOGENEOUS BEC

The TF distribution indeed appears to be a good approximation. This is demonstrated by the direct numerical simulations shown in Fig. 1 (c.f. the panels a and b). The discrepancy between the exact solution ψ_0 and the one generated by ψ_{TF} appears mainly due to the three-body collisions that are not accounted by the exact solution. The remarkable fact is that the rogue wave survives the effect of the quintic dissipative nonlinearity with the latter being responsible only for lowering the maximal amplitude and for retarding times t_m at which the maximum occurs [$t_m \approx 0.5 > 0$ in Fig. 1(b)].

This leads us to another issue, namely, the sensitivity of the effect to more general initial conditions. To study this, we consider the example of the "Mexican hat" distribution against the homogeneous background,

$$\psi_{MH} = \rho_{MH} e^{i\theta_i}, \quad |\rho_{MH}|^2 = 1 + a\left(1 - \frac{x^2}{\tilde{x}^2}\right) e^{-x^2/\tilde{x}^2}, \qquad (5)$$

where θ_i is given by Eq. (3). Such initial conditions can be created by properly adjusted laser beams having the Gaussian form. At $\tilde{x}^2 \approx 1/2 + 2t_i^2$ and $a = 8/(1+4t_i^2)$, the "Mexican hat" distribution well reproduces the desired initial distribution ρ_i given by Eq. (3) [see the inset in Fig. 1(c)]. Figure 1(c) shows the dynamics originated by ψ_{MH}. It generates a rogue wave followed by smooth small-amplitude modulations of the background.

Finally, we have found that the rogue wave can be generated with the help of pure phase engineering, where the initial density is a constant. This scenario is illustrated in Fig. 1(d), where θ_i from Eq. (3) was chosen as the initial phase distribution. We again observe the "post-rogue" evolution in the form of the modulated background, which however is slightly different from the previous cases involving density engineering.

IV. ROGUE WAVE IN A BEC LOADED IN AN OPTICAL LATTICE

Even bigger rouge waves can be observed in a BEC loaded into an OL, where it is developed from the simple Bloch wave. Such a state has two new features. First, the rogue wave is developed on the scale imposed *a priori* and determined by the lattice constant. Second, the phenomenon can be observed in a BEC with a positive scattering length. The latter does not require the use of the Feshbach resonance technique. Analysis presented in the previous section shows that the controlled excitation of the rogue waves requires two conditions to be satisfied simultaneously. These are the requirements for the modulational instability as well as special initial density and velocity distributions. The latter conditions can be provided in the case of OL in the same way as for the homogeneous condensate, i.e., using combined density engineering and phase imprinting. The conditions for modulation instability in the case of a BEC loaded in an OL are completely changed by the lattice. The reason is that any two Bloch states bordering different edges of a band gap of the linear spectrum have different stability properties. Namely, one of them is stable while another one is unstable [15]. Thus, for any sign of the scattering length one can achieve the conditions for the modulational instability just choosing correctly one of the initial states. This is the approach which we implemented in this section.

To this end, we turn to the GP equation

$$i\psi_t = -\psi_{xx} - V\cos(2x)\psi + \sigma|\psi|^2\psi - ig|\psi|^4\psi, \qquad (6)$$

which now includes a π-periodic OL with the amplitude $V > 0$. As before, we take into account the inelastic three-body interactions by including the quintic dissipative term. The chosen period of the lattice means that the spatial and temporal variables in Eq. (6) are measured in the units of d/π and $\hbar/E_R$, respectively, while the energy is measured in units of the recoil energy $E_R = \hbar^2\pi^2/(2md^2)$, where d is the lattice constant and m is the atomic mass. The 1D density distribution $|\psi|^2$ is measured in $\pi^2 a^2/(4d^2|a_s|)$ units, where a is the transverse trap width.

Let us assume that the initial density is low enough to be well described in the linear approximation with $\sigma = g = 0$. Then, the initial stationary density distribution is nothing else but one of the normalized Bloch states $\varphi_{0,1}(x)$. It is close to one of the energy gaps. We assume that the condensate is loaded into the lowest band, such that the subscripts 0 and 1 refer to its minimum (at $q=0$) and to its maximum (at $q=1$), respectively. The wavenumber q belongs to the first Brillouin zone: $|q| \leq 1$. Each Bloch state is characterized by the dispersion relation $\mathcal{E}_q$ and by the effective mass $M_q = (d^2\mathcal{E}_q/dq^2)^{-1}$.

In the presence of the nonlinearity, one of the Bloch states becomes modulationally unstable [15]. Introducing the nonlinearity coefficients $\chi_q = \sigma\int_0^\pi |\varphi_q|^4 dx$, the instability condition can be written down as $M_q\chi_q < 0$. For the chosen initial state, $M_0 > 0$ and $M_1 < 0$. Hence, for a condensate with a positive $\chi_{0,1} > 0$ (negative $\chi_{0,1} < 0$) scattering length, the unstable state occurs at the upper, $q=1$ (lower, $q=0$), edge of the first band, i.e., the Bloch state $\varphi_1(x)$ [$\varphi_0(x)$] is unstable.

Like in the homogeneous condensates, an excitation of rogue waves in OLs requires an appropriate determination of the initial phase and density distributions. This appears to be easy since the initial state can be of a very low density when it is accurately described within the framework of the multiple-scale approximation. Accordingly, we look for the order parameter in the form $\psi \approx \varepsilon A(\tau,\xi)\varphi_q(x)\exp(-i\mathcal{E}_q t_0)$ (see Ref. [15] for the details), where $q = 0, 1$, ε is a small parameter discussed below, $\tau = \varepsilon^2 t$, $\xi = \varepsilon x$, and the slowly varying amplitude $A(\tau,\xi)$ solves the NLS equation

$$iA_\tau = -(2M_q)^{-1}A_{\xi\xi} + \chi_q|A|^2A. \qquad (7)$$

Now, in analogy with Eq. (2), one can construct the exact evolution for A. This, however, will not give us a rogue wave, as the giant increase in the density, in a generic case, breaks the conditions of the applicability of the small-amplitude approximation. The approximate Eq. (7) however allows us to determine the proper initial (at $t=t_i$) condition for exciting rogue waves,

$$\psi_i = \frac{\varepsilon}{\sqrt{\chi_q}}\left(1 - 4\frac{1-(-1)^q 2i\varepsilon^2 t_i}{1+4\varepsilon^4 t_i^2 + 4|M_q|\varepsilon^2 x^2}\right) \times \varphi_q(x) e^{-i[\mathcal{E}_q + (-1)^q \varepsilon^2] t_i}. \quad (8)$$

For a given t_i, Eq. (8) contains only one free parameter ε which determines the scale of the solution. We used smooth initial modulations with various ε and performed direct numerical simulations of Eq. (6). The results are summarized in Fig. 2. We observe the emergence of the rogue waves both at the lower [Fig. 2(a)] and at the upper [Fig. 2(b)] edges of the first band. The density reaches the values ~ 0.035, i.e., almost 5.5 times higher than the initial amplitude of the modulation. Starting with the higher initial intensity results in the increase in the rogue wave amplitude by the factor of 15. This is shown in panels c and d of Fig. 2. Moreover, we can see that an array of rogue waves is generated. We again observe that the rogue wave survives the effect of strong three-body interactions [see Figs. 2(e) and 2(f)].

The theory reported above is quasi-1D, while the experimentally created BECs are three dimensional, even in the cases when cigar-shaped confining potentials are used. This raises an important question about the validity of this approximation for the description of rogue waves. More specifically, we have to establish the conditions which allow one to describe the condensate in terms of the 1D model even at the stage of maximal amplitude of the rogue wave. To argue the applicability of the theory for large regions of the governing parameters, we recall that, say, in the case of a BEC in an OL, the transverse dynamics can be neglected only when the density of the transverse kinetic energy, $\mathcal{E}_\perp = 2d^2/(\pi a)^2$, is much bigger than both the recoil energy and the energy of the two-body interactions $\mathcal{E}_{nl} = \max_{x,t}|\psi|^2$ [15] (all measured in the E_R units). For typical experimental parameters of ^{7}Li condensate with $d \sim 1$ μm, $a \sim 0.5$ μm, and $|a_s| \sim 1$ nm, we estimate that $\mathcal{E}_{nl}/\mathcal{E}_\perp \approx 0.044$, 0.38, and 0.1 in the panels (a,b), (c,d), and (e,f) of Fig. 2, respectively. Also, the characteristic time of the rogue wave, which we identify with the time where the density profile significantly exceeds the background density, can be estimated as $\Delta t \sim 11$ ms (the dimensionless time 500) and $\Delta t \sim 3$ ms (the dimensionless time 140) in panels (a,b) and (c–f) of Fig. 2, correspondingly. Furthermore, for our numerical simulations the estimate for a real number of atoms per unit cell is $n = \frac{\pi^2 a^2}{4|a_s| d}|\psi|^2$, i.e., $n \lesssim 10$. Then the peak density (i.e., the largest number of atoms in the central well) is estimated as $n_{peak} \sim 10^2$ [Figs. 2(c) and 2(d)]. Thus, with suitable choice of the parameters a rogue wave will neither cause excitation of higher transverse levels nor break the applicability of the quasi-1D mean-field approximations (however, neither of these effects is excluded in principle).

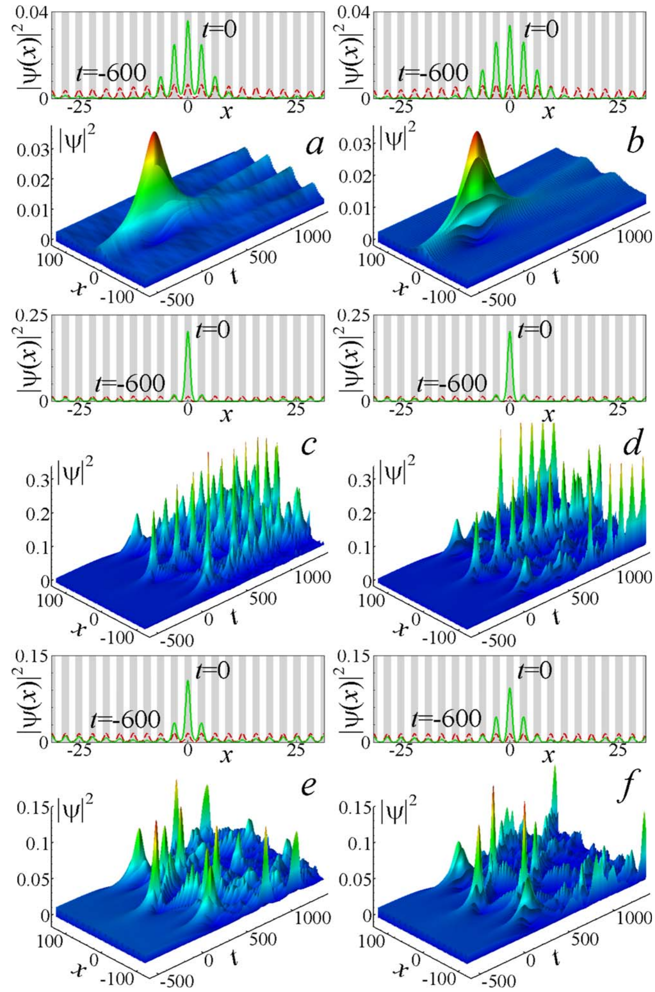

FIG. 2. (Color online) Evolution of the atomic density starting at the lower (left column, $\sigma=-1$, $E_0=-0.9368$) and upper (right column, $\sigma=1$, $E_1=-0.7332$) edges of the first lowest band of the OL with $V=3$. As the initial condition, we used Eq. (8) with $t_i=-600$ and $\varepsilon=0.05$ (panels a,b), $\varepsilon=0.1$ (panels c–f). The rogue wave is observed without dissipative losses (panels a–d) and with inelastic interactions (panels e,f, where $g=0.5$). The upper insets show the respective initial shapes at t_i (dashed lines) and ones at $t=0$, when rogue waves reach their maxima (solid lines) [gray and white strips correspond to half-periods of OL, when $-V\cos(2x)<0$ and $-V\cos(2x)>0$, respectively].

V. DISCUSSION AND CONCLUSIONS

To conclude, we reported the possibility of observation of rogue waves in BECs. While the fact that the existence of such waves is somehow evident, it follows from the fact that the mean-field dynamics of a BEC is described by the Gross-Pitaevskii equation; there exists several features of the phenomenon observed in a condensed atomic gas. First, condensates are created in the presence of an external potential, which is typically parabolic one. Second, the three-body interactions are expected to become a significant factor in the course of the evolution of the rogue waves (in our simulations they were taken into account by the quintic nonlinearity). Third, the rogue waves can be generated in a controlled manner by phase and amplitude engineering.

In homogeneous condensates, the rogue waves display local increase in the amplitude up to several times. The effect can be enhanced using optical lattices due to confining effect of the neighboring lattice maxima. In the latter case, the density amplitude can be amplified tens of times. This occurs on the scale of the lattice constant. The great advantage of the rogue waves in BECs, compared to already observed ones in the ocean and in optical systems, is that they can be manipulated using tunable interatomic interactions as well as the flexibility of the confinement and lattice potentials. Moreover, the use of the periodic potential allows one to observe rogue waves in media where homogeneous plane waves are stable. The rogue waves are remarkably stable with respect to inelastic three-body interaction. One can further predict that due to giant local increase in the density, the rogue waves can result in enhanced quantum fluctuations, in appearance of the transverse dynamics of the initially quasi-one-dimensional condensate, and even in complete destruction of the atomic condensate.

Our study here is devoted to numerical demonstrations of new effects in BEC science. We based our simulations on NLS equation as a rough approximation and confirmed numerically that basic rogue wave solution is robust and retains its features when the equation is perturbed. Clearly, this approach raises mathematical questions about stability of rogue wave solutions relative to perturbations of the initial equation. The preliminary answer is given by our simulations using different initial conditions and showing the robustness of the rogue waves. As any problem of stability, it is vastly complicated and cannot be solved in the frame of a single work. Presently, we are at the beginning stage of understanding these problems, with some results being prepared for a separate publication.

Finally, recalling that the modulational instability [15] was already observed experimentally [18] and that large diversity of the trap potentials are available experimentally [19], the rogue waves appear to be the next exciting phenomenon to look for in future experiments.

ACKNOWLEDGMENTS

Y.V.B. acknowledges partial support from FCT under Grant No. SFRH/PD/20292/2004. The work of N.A. is supported by the Australian Research Council (Discovery Project, Grant No. DP0985394).

[1] C. Kharif, E. Pelinovsky, and A. Slunyaev, *Rogue Waves in the Ocean* (Springer, Heidelberg, 2009).

[2] A. R. Osborne, *Nonlinear Ocean Waves* (Academic Press, New York, 2009).

[3] P. Müller, Ch. Garrett, and A. Osborne, Oceanogr. **18**, 66 (2005).

[4] W. Rosenthal, S. Lehner, H. Dankert, H. Guenther, K. Hessner, J. Horstmann, A. Niedermeier, J. C. Nieto-Borge, J. Schulz-Stellenfleth, and K. Reichert, *Detection of Extreme Single Waves and Wave Statistics*, Proceedings of MAXWAVE Final Meeting, October 8–10, 2003, Geneva, Switzerland (unpublished).

[5] C. Kharif and E. Pelinovsky, Eur. J. Mech. B/Fluids **22**, 603 (2003).

[6] A. R. Osborne, M. Onorato, and M. Serio, Phys. Lett. A **275**, 386 (2000); A. R. Osborne, Mar. Struct. **14**, 275 (2001).

[7] P. A. E. M. Janssen, J. Phys. Oceanogr. **33**, 863 (2003); V. V. Voronovich, V. I. Shrira, and G. Thomas, J. Fluid Mech. **604**, 263 (2008); K. B. Dysthe and K. Trulsen, Phys. Scr. **T82**, 48 (1999); P. K. Shukla, I. Kourakis, B. Eliasson, M. Marklund, and L. Stenflo, Phys. Rev. Lett. **97**, 094501 (2006).

[8] T. B. Benjamin and J. E. Feir, J. Fluid Mech. **27**, 417 (1967); V. I. Bespalov and V. I. Talanov, Pis'ma Zh. Eksp. Teor. Fiz. **3**, 471 (1966) [JETP Lett. **3**, 307 (1966)].

[9] D. H. Peregrine, J. Austral. Math. Soc. **25**, 16 (1983).

[10] N. Akhmediev, J. M. Soto-Crespo, and A. Ankiewicz, Phys. Lett. A **373**, 2137 (2009).

[11] N. Akhmediev, A. Ankiewicz, and M. Taki, Phys. Lett. A **373**, 675 (2009).

[12] D. R. Solli, C. Ropers, P. Koonath, and B. Jalali, Nature (London) **450**, 1054 (2007); D.-I. Yeom and B. Eggleton, *ibid.* **450**, 953 (2007).

[13] L. Pitaevskii and S. Stringari, *Bose-Einstein Condensation* (Oxford University Press, New York, 2003).

[14] W. C. Stwalley, Phys. Rev. Lett. **37**, 1628 (1976); E. Tiesinga, A. J. Moerdijk, B. J. Verhaar, and H. T. C. Stoof, Phys. Rev. A **46**, R1167 (1992); S. Inouye *et al.*, Nature (London) **392**, 151 (1998); J. Stenger, S. Inouye, M. R. Andrews, H. J. Miesner, D. M. Stamper-Kurn, and W. Ketterle, Phys. Rev. Lett. **82**, 2422 (1999).

[15] V. V. Konotop and M. Salerno, Phys. Rev. A **65**, 021602(R) (2002).

[16] P. O. Fedichev, M. W. Reynolds, and G. V. Shlyapnikov, Phys. Rev. Lett. **77**, 2921 (1996).

[17] L. Dobrek, M. Gajda, M. Lewenstein, K. Sengstock, G. Birkl, and W. Ertmer, Phys. Rev. A **60**, R3381 (1999); S. Burger, K. Bongs, S. Dettmer, W. Ertmer, K. Sengstock, A. Sanpera, G. V. Shlyapnikov, and M. Lewenstein, Phys. Rev. Lett. **83**, 5198 (1999); J. Denschlag *et al.*, Science **287**, 97 (2000).

[18] L. Fallani, L. De Sarlo, J. E. Lye, M. Modugno, R. Saers, C. Fort, and M. Inguscio, Phys. Rev. Lett. **93**, 140406 (2004).

[19] K. Henderson, C. Ryu, C. MacCormick, and M. G. Boshier, New J. Phys. **11**, 043030 (2009).